

Optimization of a far-off-resonance continuous-wave Raman laser

P. A. Roos, L. S. Meng, and J. L. Carlsten

Department of Physics, Montana State University, Bozeman, Montana 59717

Received May 31, 2001; revised manuscript received November 21, 2001

We derive self-contained, analytic expressions for the emitted Stokes and pump powers from a low-power, cw Raman laser. In addition to facilitating the physical understanding of these systems, the expressions lead to the conditions for laser threshold and impedance matching. Moreover, they provide the starting point for optimizing the device efficiency with respect to input pump power, mirror transmissions, two-photon detuning, and cavity geometry. We obtain simple, analytic expressions for the optimization conditions while retaining sufficient generality to include asymmetric mirror coatings as well as absorptions. These mathematical guidelines are balanced with practical issues to yield the most advantageous system operation parameters.

© 2002 Optical Society of America

OCIS codes: 140.3550, 190.2620, 190.5650.

1. INTRODUCTION

Exploiting the substantial optical power enhancement within a high-finesse optical cavity (HFC) by use of milliwatt-range pump sources has recently yielded systems that include cw Raman lasers detuned far from any single-photon transition.¹⁻⁵ The first of these systems used a highly stabilized, frequency doubled Nd:YAG laser as the pump source,^{1,2} but diode lasers have subsequently been used because of their relative low cost, broad spectral coverage, and tunability.^{3,4} Together, these devices have demonstrated linewidths of less than 10 kHz,² thresholds below 0.5 mW,³ discrete tuning of 40 nm,⁴ and greater than 1.5-GHz continuous tuning⁵ as well as the extremely high spatial purity generated by a nonconfocal, high-finesse laser resonator. With currently available room-temperature diode lasers as the pumps, the Stokes-shifted output is predicted to extend from the visible past 5 μm . Such properties make cavity-enhanced cw Raman lasers attractive for a variety of applications, including high-resolution spectroscopy, remote sensing, atomic physics, and possibly telecommunications.

Early theoretical predictions for cw Raman lasing in the focused geometry were made by Boyd *et al.*⁶ Their study, based on amplifier theory, treats a system for which only the Stokes field is enhanced by a cavity but whose extension to the doubly resonant case, in which the cavity mirrors are highly reflective at both the pump and the Stokes wavelengths, is straightforward. They derived the conditions for laser threshold including the effects of beam diffraction and showed that the maximum Raman gain per pass is realized when the confocal parameters for the pump and the Stokes modes are equal. More recently, as a result of the experimental realization of far-off-resonance cw Raman lasers, increased attention has been focused on theoretical descriptions of such systems.^{2,7-10} In the research reported in Ref. 7 a steady-state interferometric approach was used that involved a depleted intracavity pump field that was due to Raman conversion. That research gives numerical

guidelines for choosing the mirror reflectivities when the two resonator mirrors are identical and shows that the maximum photon conversion efficiency, 50%, occurs at a pump power that is four times the threshold value. Identical characteristics for nondegenerate optical parametric oscillators (NDOPOs) above threshold follow directly from early studies by Siegman.¹¹ In Ref. 8 the treatment is extended to describe the improved conversion efficiency that one can realize by dropping the input coupler reflectivity of the HFC. It is shown that photon conversion efficiency can approach 100% with the proper choice of mirror reflectivities. Rebic *et al.*⁹ treated the transfer of nonclassical photon statistics from the input pump to the output Stokes. Their steady-state results differ from those of this research and of the other research referred to here because of their assumption that the pump cycle is closed coherently. Petersen *et al.*¹⁰ developed a steady-state treatment based on amplifier theory. These researchers have shown that a reduction in the mirror reflectivities can lead to greater power extraction, thereby reinforcing the findings presented in Ref. 7. Brasseur *et al.*² developed a time-dependent field theory based on Lamb's self-consistency equations.¹² They compared both the time-dependent and the steady-state limit results with experimental data.

In the present study we aim to extend the research of Ref. 2 and then, from both a mathematical and a practical standpoint, to thoroughly treat the issue of optimizing a low-power cw Raman laser system based on a linear cavity geometry. The treatments given in Ref. 2 and in this paper are unsuitable for systems in which thermal lensing is significant but have been shown to give good agreement with experimental data for our systems that generate less than ~ 5 mW of Stokes optical power over an ~ 3 -in. (~ 7.6 -cm) cavity length. We also assume a high finesse limit throughout and that longitudinal variations of the fields within the cavity can be neglected. In this form the theory is therefore unsuitable for Raman shifting in long fibers, for which the single-pass conversion can

be significant. By developing completely analytic optimization conditions, we hope that this study can facilitate understanding of cw Raman systems as well as provide guidelines for determining the optimal parameters for construction and operation of such devices. Specifically, we address choices of input pump power, resonator mirror transmissions at both pump and Stokes wavelengths, two-photon detuning, cavity length, and mirror curvature.

This paper is organized in the following manner: In Section 2 we extend the theoretical work of Ref. 2 to produce analytic expressions for the steady-state reflected and transmitted pump powers as well as the output Stokes power from the cw Raman laser. We use these expressions to generate the input pump powers required for laser threshold and impedance matching. In Section 3 we differentiate these expressions with respect to the input pump power and, in Section 4, the resonator transmission coefficients to determine the optimal parameters. We include mirror absorptions in this optimization procedure, and it is performed for symmetric mirrors (meaning that the front and the back mirrors are identical) as well as for asymmetric mirrors (meaning that the front and the back mirrors have different reflectivities).⁸ In Sections 5 and 6 we investigate the optimal detuning from the two-photon Raman resonance line center, and we discuss considerations associated with the most advantageous resonator length and mirror curvature. The final section consolidates our findings and provides some concluding thoughts.

2. STEADY-STATE POWERS

We begin by extending the theoretical treatment given in Ref. 2. From the groundwork laid in that paper we generate self-contained analytic expressions for the steady-state powers emitted and reflected from the resonator as functions of the input pump power. The pump powers required for threshold and for impedance matching then follow immediately. This treatment does not include the power dependence of propagation constants (i.e., thermal lensing and gain guiding),^{13,14} nor does it treat depletion of the Raman gain medium. Inclusion of these additional effects necessitates numerical solutions and is a current topic of investigation.¹⁵

One can convert the field equations given in Ref. 2 to optical powers that are external to the resonator, as shown, for example, in Appendix A. After these algebraic manipulations the following analytic expressions can be obtained for the pump optical powers reflected from (front) and transmitted through (back) the resonator as well as for the Stokes optical power exiting the Raman resonator above threshold:

$$P_{P_f} = \left\{ \left[\frac{1}{4} P_1 T_{P_f} (1 - \sqrt{R_{S_f} R_{S_b}}) \right]^{1/2} - \sqrt{P_{\text{In}}} \right\}^2, \quad (1)$$

$$P_{P_b} = 1/4 P_1 T_{P_b} (1 - \sqrt{R_{S_f} R_{S_b}}), \quad (2)$$

$$P_{S_{f(b)}} = \frac{1}{2} \frac{\lambda_P}{\lambda_S} T_{S_{f(b)}} \left[\left(\frac{T_{P_f}}{1 - \sqrt{R_{S_f} R_{S_b}}} P_1 P_{\text{In}} \right)^{1/2} - \frac{1}{2} P_1 (1 - \sqrt{R_{P_f} R_{P_b}}) \right]. \quad (3)$$

In the equations in this paper the subscripts P and S refer to the pump and the Stokes waves and the subscripts f and b refer to the front (input) and the back of the resonator, respectively. P_{In} is the input pump optical power (note that this is the *coupled* pump power into the resonator), λ represents an optical wavelength, R and T represent power reflection and transmission coefficients, respectively, and we have defined the following constant with units of power:

$$P_1 \equiv \frac{\lambda_P + \lambda_S}{2 \alpha_0 \csc^{-1} \sqrt{2r/l}}. \quad (4)$$

In Eq. (4), α_0 is the plane-wave gain coefficient at line center for the Raman transition,¹⁶ r is the radius of curvature of the resonator mirrors, and l is their separation. Physically, $P_1/2$ represents the pump power that gives an exponential gain of unity per pass based on amplifier theory.¹⁷ The results given above are consistent with energy conservation and can also be derived from the steady-state treatments of Repasky *et al.*^{7,8} (if the factor-of-2 discrepancy in the gain is accounted for, as mentioned in Ref. 2) and of Peterson *et al.*¹⁰ in the limit of small single-pass gain ($\eta S_{\text{out}} \ll 1$) and high finesse. Additionally, we note that the radical signs involving the mirror reflectivities in Eqs. (1)–(3) can be eliminated by use of the approximation $1 - \sqrt{x} \approx (1 - x)/2$, which is valid when $x \approx 1$.

Equation (3) shows that the Stokes power grows as the square root of the incident pump power after threshold, as with the downconverted power of a cw NDOPO.¹¹ The Raman laser threshold occurs when the two terms within the brackets are equal. Explicitly, the threshold input pump power is

$$P_{\text{Thresh}} = \frac{1}{4} P_1 (1 - \sqrt{R_{S_f} R_{S_b}}) \frac{(1 - \sqrt{R_{P_f} R_{P_b}})^2}{T_{P_f}} \approx \frac{\pi^2}{4} \frac{P_1}{F_P F_S}, \quad (5)$$

where F_P and F_S are the cavity finesesses at the pump and the Stokes wavelengths, respectively, and the approximate equality holds only for the case of symmetric mirrors. This result emphasizes the advantage of doubly resonant systems because the threshold is reduced by the product of the two cavity finesesses.

Equation (2) shows that, above threshold, the transmitted pump power is independent of the input pump power, as with a NDOPO.¹¹ Its value is clamped to that of the empty cavity transmission at the onset of lasing. This clamping behavior also critically affects the total reflected pump power from the resonator, given by Eq. (1). The first term within the braces can be compared directly to

Eq. (2) and is associated with the field that is transmitted out the front of the HFC (depending on the Raman medium), whereas the second term within the braces is associated with the portion of the incident field reflected from the HFC input coupler (independently of the Raman medium). These two fields combine out of phase, yielding a total reflected power from the active cavity that depends nonlinearly on the input pump power. Such reflections from active cavities are commonly observed in cavity-enhanced nonlinear systems (see Ref. 18 and references therein). To achieve impedance matching (zero total reflected power) we can equate the two terms within braces of Eq. (1). Solving for the pump power then yields

$$P_{\text{Matched}} = 1/4P_1(1 - \sqrt{R_{S_f}R_{S_b}})T_{P_f} \quad (6)$$

$$= \frac{1}{\left(1 + \frac{A_P}{T_P}\right)^2} P_{\text{Threshold}} \quad (R_{P_f} = R_{P_b}) \quad (7)$$

$$= \frac{4}{\left(1 + \frac{\Lambda_P}{T_{P_f}}\right)^2} P_{\text{Threshold}} \quad (R_{P_f} \ll R_{P_b}), \quad (8)$$

where $\Lambda_P = T_{P_b} + A_{P_b} + A_{P_f}$ and represents the effective pump losses in the system (i.e., those losses that degrade system's conversion efficiency). We have used the relation $R + T + A = 1$, and to obtain Eq. (8) we have performed a Taylor expansion, retaining only terms that are linear in T and A . When the front and the back resonator mirrors are identical, Eq. (7) shows that the impedance matching condition is never achieved above threshold but approaches $P_{\text{Threshold}}$ when $T_P \gg A_P$. However, as input coupler reflectivity R_{P_f} is decreased the pump power required for impedance-matching rises above threshold and approaches $4 \times P_{\text{Threshold}}$ in the limit $T_{P_f} \gg T_{P_b} + A_{P_b} + A_{P_f}$, as shown by Eq. (8). This indicates that more pump light can enter the HFC for Raman conversion when the input coupler's reflection coefficient is much lower than that for the back mirror at the pump wavelength. Interestingly, however, as is shown in Section 3, the optical power required for impedance matching does not, in general, correspond exactly to that which produces the greatest conversion efficiency.

3. OPTIMAL INPUT PUMP POWER

Now we begin directly optimizing the low-power cw Raman system. We can solve for the photon conversion efficiency by dividing Eq. (3) by the input pump power. Differentiating the result with respect to the input pump power and equating to zero yield $P_{\text{In}} = 4 \times P_{\text{Threshold}}$. The maximum conversion efficiency occurs at four times threshold, regardless of mirror reflectivities, resonator geometry, or Raman plane-wave gain coefficient, confirming the result introduced by Repasky *et al.*⁷ It is interesting to note that exact impedance matching from Section 2 does not occur at the same pump power as the peak conversion efficiency but approaches it in the limit of small effective losses. Using an input pump power of $P_{\text{In}} = 4$

$\times P_{\text{Threshold}}$, one can easily show that the photon conversion efficiency reaches a maximum value of

$$\frac{P_{S_b} \lambda_S}{P_{\text{In}} \lambda_P} = \frac{1}{4} \frac{T_{S_b} T_{P_f}}{(1 - \sqrt{R_{S_f} R_{S_b}})(1 - \sqrt{R_{P_f} R_{P_b}})}. \quad (9)$$

For the symmetric mirror case, when light emitted from both ends of the resonator is included, this result simplifies to

$$\frac{P_S \lambda_S}{P_{\text{In}} \lambda_P} = \frac{1}{2} \frac{1}{\left(1 + \frac{A_S}{T_S}\right)\left(1 + \frac{A_P}{T_P}\right)}, \quad (10)$$

which approaches 50% in the limit of small absorptions. And when the reflectivity of the input coupler is decreased, thereby raising the impedance-matching power, the maximum conversion efficiency from Eq. (9) becomes

$$\frac{P_{S_b} \lambda_S}{P_{\text{In}} \lambda_P} = \frac{1}{\left(1 + \frac{\Lambda_S}{T_{S_b}}\right)\left(1 + \frac{\Lambda_P}{T_{P_f}}\right)}, \quad (11)$$

where $\Lambda_S = T_{S_f} + A_{S_f} + A_{S_b}$ and $\Lambda_P = T_{P_b} + A_{P_b} + A_{P_f}$. This result shows that a photon conversion efficiency approaching 100% can be achieved in the output from a single end of the resonator in the limit of small losses, in agreement with Ref. 8. Note also that with the asymmetric mirror the transmission of the front mirror at the Stokes wavelength and that of the back mirror at the pump wavelength enter as losses equivalent to the mirror absorptions.

The simplicity of results (10) and (11) highlight their significance. That is, the only parameters that degrade the maximum conversion efficiency are the (effective) resonator losses that are relative to the transmissions at the two wavelengths. Other losses in the system, such as Rayleigh and other scattering mechanisms, can be included in the effective absorption terms. We do not address the residual birefringence of the mirrors used in the HFC or warping that is due to heat deposition.¹⁹ Polarization rotation of the transmitted pump field relative to the field reflected from the input coupler as a result of mirror birefringence will result in incomplete interference and therefore in coupling losses into the Raman resonator. Self-defocusing from a radial thermal gradient can also alter the coupling efficiency.¹⁵ Most of these effects can be avoided by generation of a relatively small amount of Stokes power output.

4. OPTIMAL MIRROR TRANSMISSION COEFFICIENTS

We now treat the case in which the maximum amount of available pump power is a known parameter (we hold P_{In} fixed) and we wish to maximize Stokes power extraction or, equivalently, the photon conversion efficiency with an appropriate choice of mirror transmissions. One might expect that we would simply want to choose mirrors such that the threshold occurs at one quarter of the available

pump power (i.e., satisfies the four-times-threshold condition). However, in this section we show that such is not necessarily the case.

For identical front and back mirrors and when absorptions are negligible, Eq. (3) can be simplified to show that the resonator mirror transmissions at the pump and the Stokes wavelengths enter symmetrically and as a product. It is therefore not advantageous to make the mirror transmission at one wavelength higher than at the other. For this case it can be shown that there exists a family of optimal mirror transmission coefficients whose product satisfies

$$T_S T_P = P_{In}/P_1. \quad (12)$$

This transmission product yields $P_{Thresh} = P_{In}/4$ from approximation (5) and a conversion efficiency of 50%. So, in the absence of absorptions, the maximum Stokes power is achieved by selection of mirror reflectivities such that the four-times-threshold condition is achieved for the fixed available input pump power, P_{In} .

However, when absorptions are included, such is no longer the case. Differentiating Eq. (3) with respect to each transmission coefficient, equating to zero, and solving the resulting two equations simultaneously yield the following optimization conditions for the symmetric mirror case:

$$T_P = \left(\frac{A_P P_{In}}{A_S P_1} \right)^{1/2}, \quad (13)$$

$$T_S = \left(\frac{A_S P_{In}}{A_P P_1} \right)^{1/2} - A_S. \quad (14)$$

These relations indicate that different mirror transmissions at the two wavelengths will, in general, be required for optimizing the Stokes output power. Inserting the optimal transmissions given by Eqs. (13) and (14) into Eq. (3) and converting to photon conversion efficiency yield

$$\frac{P_S \lambda_S}{P_{In} \lambda_P} = \frac{1}{2} \left[1 - \left(\frac{P_1}{P_{In}} A_P A_S \right)^{1/2} \right]^2. \quad (15)$$

The most favorable conditions exist when the product of absorptions is small but also when P_1/P_{In} is minimized. In the limit where both absorptions are zero, the efficiency is again the ideal 50%.

For the asymmetric mirror it can be seen from Eq. (11), and shown more rigorously, that the back pump mirror and the front Stokes mirror reflection coefficients should be as high as possible. We therefore treat only T_{P_f} and T_{S_b} as variable parameters in Eq. (3) for maximization. The equations analogous to Eqs. (13)–(15) for the asymmetric case then become

$$T_{P_f} = \left(\frac{\Lambda_P 8P_{In}}{\Lambda_S P_1} \right)^{1/2}, \quad (16)$$

$$T_{S_b} = \left(\frac{\Lambda_S 8P_{In}}{\Lambda_P P_1} \right)^{1/2} - \Lambda_S, \quad (17)$$

$$\frac{P_{S_b} \lambda_S}{P_{In} \lambda_P} = \left[1 - \left(\frac{P_1}{8P_{In}} \Lambda_P \Lambda_S \right)^{1/2} \right]^2. \quad (18)$$

Again, the conversion efficiency is degraded by the (effective) loss terms, Λ_P and Λ_S , and again the existence of these losses leads to an asymmetry between the mirror reflection coefficients at the two wavelengths for optimal Stokes power extraction.

Figure 1 shows the Stokes output power as a function of the Stokes transmission coefficient on the horizontal axis and the pump transmission coefficient on the vertical axis for the symmetric mirror case with $A_p = A_s$. The lowest contour bounds the region of transmission parameter space in which lasing can occur. Note the asymmetry that is reflective of Eqs. (13) and (14). The maximum

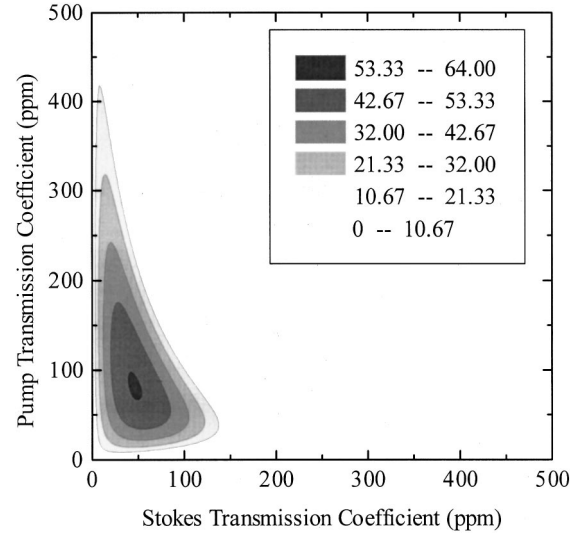


Fig. 1. Output Stokes power (arbitrary units) from Eq. (1) as a function of the mirror transmission coefficients [in parts in 10^6 (ppm)] at the pump and Stokes wavelengths for equal absorption coefficients of 35 ppm. Note that the optimal Stokes transmission coefficient is lower than that for the pump. The other parameters used for Figs. 1–3 are $P_1 = 0.44$ MW, $\lambda_p = 795$ nm, and $\lambda_s = 1187$ nm.

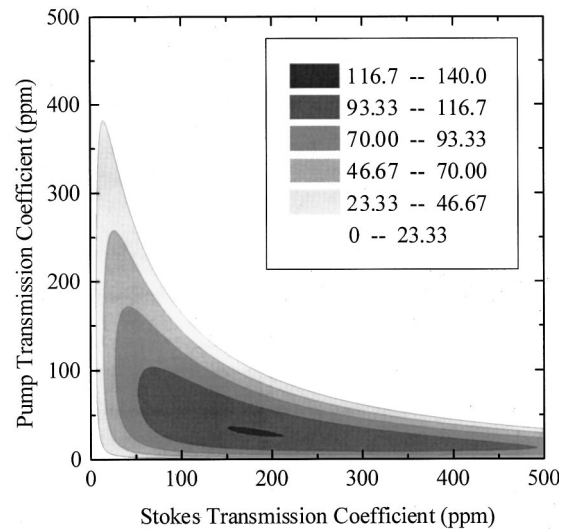


Fig. 2. Output Stokes power (arbitrary units) from Eq. (1) as a function of the mirror transmission coefficients (ppm) at the pump and the Stokes wavelengths when the absorption coefficient for the pump wavelength is smaller (5 ppm) than that for the Stokes wavelength (35 ppm). Here the optimal Stokes transmission is larger, whereas that for the pump decreases.

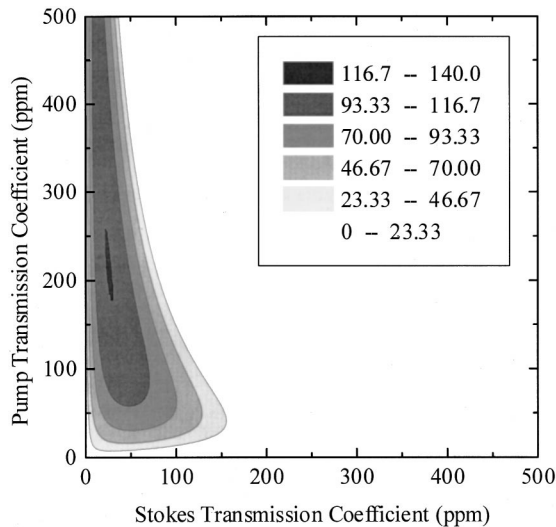


Fig. 3. Output Stokes power (arbitrary units) from Eq. (1) as a function of the mirror transmission coefficients (ppm) at the pump and the Stokes wavelengths when the absorption coefficient for the pump wavelength (35 ppm) is larger than that for the Stokes wavelength (5 ppm). For this case the optimal Stokes transmission decreases and that for the pump increases.

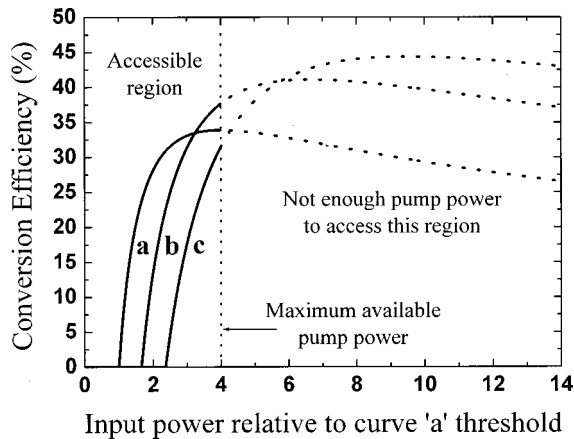


Fig. 4. Photon conversion efficiency as a function of input pump power relative to the threshold power of curve a. We assume that the accessible pump powers are limited to the region to the left of the vertical dotted line. Curve a shows the efficiency when the mirror transmissions are chosen such that the maximum available pump power is four times the threshold pump power. Curve b shows the efficiency when the transmissions increase to match Eqs. (13) and (14) of Section 4. Curve c shows the efficiency for even larger transmissions.

output power occurs when the Stokes transmission coefficient is lower than that of the pump. Figures 2 and 3 show the conditions when $A_S > A_P$ and $A_P > A_S$, respectively, for the symmetric mirrors.

It is interesting to note, however, that when the above optimal transmission coefficients are used the Raman laser threshold does not occur at $P_{In}/4$. Instead, it can be shown that the threshold is pushed to a larger fraction of P_{In} . For symmetric mirrors the threshold that corresponds to the optimal mirror transmissions occurs at

$$P_{\text{Threshold}} = \frac{P_{\text{In}}}{4} \left[1 + \left(\frac{P_1}{P_{\text{In}}} A_P A_S \right)^{1/2} \right]^2. \quad (19)$$

This result seems to contradict the assertion above that the maximum conversion efficiency occurs at four times threshold regardless of absorption. However, the four-times-threshold condition optimizes the conversion efficiency with respect to pump power rather than to mirror transmissions. It is true that, given a set of mirrors, if sufficient optical power is available to reach four times threshold, clearly this should be done. However, with this same amount of pump power we could have produced a greater amount of Stokes power by choosing mirrors with higher transmission coefficients, thereby raising the threshold beyond $P_{In}/4$. Physically this can be interpreted as the systems' surrendering the four-times-threshold condition in exchange for a lower A/T ratio from Eq. (10).

To clarify this effect further, we show in Fig. 4 the photon conversion efficiency as a function of relative input pump power for several choices of mirror transmissions but for identical absorptions. The vertical dotted line represents the maximum available pump power. Pump powers greater than this (shown as dotted curves) cannot be realized by the system. Curve a represents the conversion efficiency that one can achieve by choosing the mirror transmission coefficients such that $P_{\text{Thresh}} = P_{In}/4$, and curve b represents the efficiency with transmissions from Eqs. (13) and (14). Curve c represents the efficiency when even higher transmissions are used. Although curve b does not reach the four-times-threshold condition for the maximum available pump power, higher conversion efficiency, meaning more Stokes power, can still be achieved. Note that one cannot realize this benefit by raising the threshold by other means, such as increasing the cavity length or detuning from two-photon Raman resonance. We wish to point out, however, that this effect is prominent only when the absorption losses in the HFC are comparable to or larger than the transmissions. We purchase our mirrors from Research Electro-Optic (REO) in Boulder, Colorado. REO can currently coat mirrors with transmission accuracy better than 5% and with absorptions typically less than several parts in 10^6 at the 800-nm wavelength.

Practical issues are perhaps particularly significant when one is choosing mirror reflectivities. Equations (13), (14), (16), and (17) indicate that, for equal absorption at the two wavelengths, to optimize the system the Stokes transmission coefficient should be lower than that for the pump. This condition is advantageous for practical reasons regardless of conversion efficiency optimization. Specifically, it is desirable to minimize the bandwidths of instabilities within the cavity that are associated with Stokes generation, such as thermal effects^{20,21} and relaxation oscillations.² From a practical standpoint, one should therefore maximize the pump HFC linewidth (reflectivity) relative to that of the Stokes. However, this benefit must be weighed against the decreased conversion efficiency realized by dropping T_s with respect to A_s in Eq. (10).

5. OPTIMAL DETUNING

To this point, we have assumed that the pump and the Stokes fields are simultaneously resonant in the cavity

and that the frequency difference between the two modes corresponds precisely to the line center of the two-photon Raman resonance. In this section we use detuning from the Raman resonance line center as a parameter to vary the power constant P_1 . For operation of a cw Raman laser with a pump power above the four-times-threshold condition (above the peak in the conversion efficiency), such detuning actually increases the output Stokes power and therefore the conversion efficiency, as was demonstrated in Ref. 5. In the high-pressure limit²² we can assume that the Raman resonance is described by a Lorentzian profile. In this case, formulas (1)–(19) are valid, with the modification that $P_1 \rightarrow P_1/L$, where

$$L = \frac{(\Gamma/2)^2}{\Delta^2 + (\Gamma/2)^2}. \quad (20)$$

Here Γ is the full width at half-maximum of the Raman transition linewidth and Δ is the detuning from the two-photon Raman resonance line center. Plots for the resulting tuning behavior can be found in Ref. 5. Differentiating the modified version of Eq. (3) with respect to this detuning, we find three roots that maximize the conversion efficiency. The first root is zero detuning, which represents a local minimum for pump powers greater than four times threshold and a global maximum for pump powers below this value. The remaining two roots maximize the conversion efficiency during operation above four times threshold:

$$\Delta = \pm \frac{\Gamma}{2} \left(\frac{P_{\text{In}}}{4P_{\text{Thresh}}} - 1 \right)^{1/2}, \quad (21)$$

where P_{Thresh} is given by approximation (5). Below four times threshold, these roots are not real, and the conversion efficiency is maximized at line center. Above four times threshold, detuning effectively decreases the Raman gain and therefore raises the laser threshold until the four-times-threshold condition is again realized for the higher pump power value. Therefore when the laser is operated with a pump power of eight times threshold, for instance, the optimal detuning is to either half-width of the Raman resonance.

6. OPTIMAL RESONATOR PARAMETERS

The optimal conditions discussed thus far can be achieved, in principle, with a Raman laser resonator of any length. This property has intriguing implications regarding the creation of compact Raman laser systems. Mathematically, the resonator length enters through the power constant of Eq. (4), but the relevant parameters is the unitless ratio of the mirror curvature to this length. From the standpoint of minimizing the threshold, and from Eqs. (15) and (18), it is most desirable that power constant P_1 be small. Ostensibly we therefore wish to choose an r/l ratio that maximizes the inverse cosecant function in Eq. (4). This function is plotted versus r/l and two well-known cavity geometries are indicated with circles in Fig. 5. The function displays a maximum value of $\pi/2$ for the concentric condition $r/l = 1/2$. For ratios

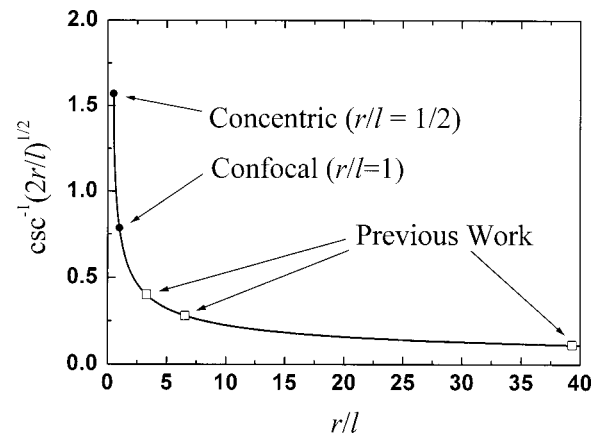


Fig. 5. Inverse cosecant function of Eq. (4) as a function of the ratio of the mirror curvature radius to the resonator length. The two filled circles mark ratios that represent familiar cavity geometries. The open squares represent ratios that we have used experimentally. The ostensibly optimal ratio is 1/2, indicating a concentric cavity geometry. However, practical considerations favor larger ratios.

less than this, the resonator is unstable.²³ The squares in this figure indicate the ratios that we have used experimentally.

There are, however, some important practical considerations when one is choosing a resonator length. The most significant of these may be that, as the resonator approaches the concentric geometry, the beam waist at the mirror surface grows rapidly.²³ This rapidly increasing beam waist can significantly degrade the finesse of the resonator not only because of diffraction losses but also as a result of mirror surface imperfections. The second concern is that, for r/l ratios that are whole number fractions, higher-order spatial modes of the interferometer will resonate at the same frequencies as the longitudinal modes.²³ This degeneracy can compromise the spatial quality of the output beam and can also degrade the finesse, not to mention the parametric coupling between modes.⁶

All the length ratios that we used experimentally have been larger than that for the concentric cavity by at least a factor of 6. It is therefore possible to reduce the thresholds of our systems by increasing the resonator lengths. We have not experimentally investigated the deleterious effects associated with smaller ratios. We suggest that one choose a resonator length that is most appropriate for the particular application with respect to free spectral range and physical size. Note that the larger the free spectral range, the more difficult it will be to achieve the doubly resonant condition for the pump and Stokes fields. A mirror curvature radius can then be selected that is longer than the resonator length. Note finally that the mirror curvature will also affect the transverse cavity mode spacing and therefore may affect the continuous tuning characteristics of the system, as discussed in Ref. 5.

7. CONCLUSIONS

Extending the steady-state limit of the time-dependent cw Raman equations introduced in Ref. 2, we have con-

firmed earlier findings that the peak conversion efficiency occurs for a pump power equal to four times the threshold value. However, we have also shown that, in the presence of losses, it is mathematically beneficial to choose mirror transmission coefficients that leave the system under the four-times-threshold value when the maximum input pump power is used. Furthermore, the optimal conditions are achieved, in general, for dissimilar transmission (or, equivalently, reflection) coefficients at the pump and Stokes wavelengths. If the system does exceed the four-times-threshold barrier, the detuning from the Raman resonance line center is derived to optimize the conversion efficiency. Practical considerations were addressed for the choice of transmission coefficients and the optimal detuning. We also found that, ostensibly, longer cavity lengths with respect to the mirror curvature were preferable but that practical considerations favor other geometries.

For most cases, one may wish to target the system operation between six and eight times threshold when the maximum available (coupled) input pump power is used. This choice of operating condition, although it is not optimized with respect to mirror reflectivities, typically allows for ample margin for error in high-reflectivity mirror coatings, and it allows for relatively constant continuous frequency tuning of the Stokes output. The mirror reflectivities should be chosen to maximize the pump cavity linewidth (decrease R_p relative to R_s) while preserving an acceptable conversion efficiency from Eq. (10). The larger pump HFC linewidth will minimize the bandwidth of instabilities associated with Stokes generation. However, for systems in which the absorptions are comparable to or larger than the transmissions and output power is the most important parameter, the system can be designed to operate below the four-times-threshold condition, as described in Section 4.

APPENDIX A

Here we derive Eq. (1) of Section 2. Equations (2) and (3) are derived in an analogous manner. We begin with the boundary conditions given by Eq. (9a) of Ref. 2 that describes the total reflected field from the input coupler mirror of the cavity in steady state:

$$E_{P_{\text{ssf}}} = -\sqrt{R_p}E_{P_{\text{in}}} + 1/2\sqrt{T_p}E_{P_{\text{ss}}}, \quad (\text{A1})$$

where $E_{P_{\text{in}}}$ is the incident and $E_{P_{\text{ss}}}$ is the intracavity pump field amplitude. The total reflected field from the cavity is a combination of the portion of the incident input field reflected from the input coupler [first term on the right-hand side of Eq. (A1)] and the portion of the intracavity pump field that is transmitted through the input coupler (second term on the right). We are free to choose the phase of the input field such that all the field amplitudes in Eq. (A1) are real, but we require that the reflected and transmitted fields be 180° out of phase. The fields in Eq. (A1) can then be converted to optical powers by use of the form

$$E = \left(\frac{2P}{A} \sqrt{\frac{\mu_0}{\epsilon_0}} \right)^{1/2}, \quad (\text{A2})$$

after Eq. (11) of Ref. 2, where A is the scaled area defined in that reference and P is the optical power associated with each field E . In terms of optical power, Eq. (A1) then becomes

$$P_{P_f} = (1/2\sqrt{T_p}\sqrt{\Pi_P} - \sqrt{R_p}\sqrt{P_{\text{In}}})^2, \quad (\text{A3})$$

where Π_P is the intracavity pump power and P_{In} is the input pump power outside the cavity.

Above threshold, the intracavity pump field is clamped and given by Eq. (6) of Ref. 2. Using that equation with Eqs. (3), (4), and (11) from Ref. 2 gives

$$\Pi_P = \frac{\lambda_P + \lambda_S}{2\alpha_0 \tan^{-1}\left(\frac{l}{b}\right)} (1 - \sqrt{R_{S_f}R_{S_b}}), \quad (\text{A4})$$

where α_0 is the Raman plane-wave gain coefficient on line center, l is the cavity length, and b is the confocal parameter. Inserting Eq. (A4) into Eq. (A3), realizing that R is nearly unity, and using the trigonometric relation²⁴

$$\csc^{-1}(x) = \tan^{-1}\left(\frac{1}{\sqrt{x^2 - 1}}\right),$$

we arrive at Eq. (1) of Section 2.

ACKNOWLEDGMENTS

We thank Jay Brasseur for essential discussions regarding this research. This research is supported by National Science Foundation grant 0097222.

The authors' e-mail addresses are, in order, roos@physics.montana.edu, meng@physics.montana.edu, and carlsten@physics.montana.edu.

REFERENCES

1. J. K. Brasseur, K. S. Repasky, and J. L. Carlsten, "Continuous-wave Raman laser in H_2 ," *Opt. Lett.* **23**, 367–369 (1998).
2. J. K. Brasseur, P. A. Roos, K. S. Repasky, and J. L. Carlsten, "Characterization of a continuous wave Raman laser in H_2 ," *J. Opt. Soc. Am. B* **16**, 1305–1312 (1999).
3. P. A. Roos, J. K. Brasseur, and J. L. Carlsten, "Diode-pumped nonresonant continuous-wave Raman laser in H_2 with resonant optical feedback stabilization," *Opt. Lett.* **24**, 1130–1132 (1999).
4. L. S. Meng, K. S. Repasky, P. A. Roos, and J. L. Carlsten, "Widely tunable continuous-wave Raman laser in H_2 pumped by an external cavity diode laser," *Opt. Lett.* **25**, 472–474 (2000).
5. J. K. Brasseur, P. A. Roos, L. S. Meng, and J. L. Carlsten, "Frequency tuning characteristics of a continuous-wave Raman laser in H_2 ," *J. Opt. Soc. Am. B* **17**, 1229–1232 (2000).
6. G. D. Boyd, W. D. Johnston, Jr., and I. P. Kaminow, "Optimization of the stimulated Raman scattering threshold," *IEEE J. Quantum Electron.* **QE-5**, 203–206 (1969).
7. K. S. Repasky, J. K. Brasseur, L. S. Meng, and J. L. Carlsten, "Performance and design of an off-resonant continuous-wave Raman laser," *J. Opt. Soc. Am. B* **15**, 1667–1673 (1998).
8. K. S. Repasky, L. S. Meng, J. K. Brasseur, J. L. Carlsten, and R. C. Swanson, "High-efficiency, continuous-wave Raman lasers," *J. Opt. Soc. Am. B* **16**, 717–721 (1999).

9. S. Rebic, A. S. Parkins, and D. F. Walls, "Transfer of photon statistics in a Raman laser," *Opt. Commun.* **156**, 426–434 (1998).
10. P. Peterson, A. Gavrielides, and M. P. Sharma, "Modeling of high finesse, doubly resonant cw Raman lasers," *Opt. Commun.* **160**, 80–85 (1999).
11. A. E. Siegman, "Nonlinear optical effects: an optical power limiter," *Appl. Opt.* **1**, 739–744 (1962).
12. W. E. Lamb, Jr., "Theory of an optical maser," *Phys. Rev.* **134**, A1429–A1450 (1964).
13. H. Kogelnik, "On the propagation of Gaussian beams of light through lenslike media including those with a loss or gain variation," *Appl. Opt.* **4**, 1562–1569 (1965).
14. B. N. Perry, P. Rabinowitz, and M. Newstein, "Wave propagation in media with focused gain," *Phys. Rev. A* **27**, 1989–2001 (1983).
15. J. Bienfang, W. Rudolph, P. A. Roos, L. S. Meng, and J. L. Carlsten, "Steady state thermo-optic model of a continuous-wave Raman laser," *J. Opt. Soc. Am. B* (to be published).
16. W. K. Bischel and M. J. Dyer, "Wavelength dependence of the absolute Raman gain coefficient for the $Q(1)$ transition in H_2 ," *J. Opt. Soc. Am. B* **3**, 677–682 (1986).
17. P. Rabinowitz, A. Stein, R. Brickman, and A. Kaldor, "Stimulated rotational Raman scattering from *para*- H_2 pumped by a CO_2 TEA laser," *Opt. Lett.* **3**, 147–148 (1978).
18. M. K. Oshman and S. E. Harris, "Theory of optical parametric oscillation internal to the laser cavity," *IEEE J. Quantum Electron.* **QE-4**, 491–502 (1968).
19. D. Jacob, M. Vallet, F. Bretenker, and A. Le Floch, "Supermirror phase anisotropy measurement," *Opt. Lett.* **20**, 671–673 (1995).
20. P. A. Roos, J. K. Brasseur, and J. L. Carlsten, "Intensity-dependent refractive index in a nonresonant cw Raman laser that is due to thermal heating of the Raman-active gas," *J. Opt. Soc. Am. B* **17**, 758–763 (2000).
21. J. K. Brasseur, R. T. Teehan, R. J. Knize, P. A. Roos, and J. L. Carlsten, "Phase and frequency stabilization of a pump laser to a Raman active resonator," *IEEE J. Quantum Electron.* **37**, 1075–1083 (2001).
22. J. R. Murray and A. Javan, "Effects of collisions on Raman line profiles of hydrogen and deuterium gas," *J. Mol. Spectrosc.* **42**, 1–26 (1972).
23. A. Yariv, *Quantum Electronics*, 3rd ed. (Wiley, New York, 1989) pp. 143–146.
24. D. Zwillinger, ed., *Standard Mathematical Tables and Formulae*, 30th ed. (CRC, New York, 1996), p. 467.